Hierarchical structure in sharply divided phase space for the piecewise linear map

Akira Akaishi,[1,*] Kazuki Aoki,[2] and Akira Shudo[2]

[1]*Department of Engineering Science, The University of Electro-Communications, 1-5-1 Chofugaoka Chofu Tokyo 182-8585, Japan*
[2]*Department of Physics, Tokyo Metropolitan University, Minami-Osawa Hachioji, Tokyo 192-0397, Japan*

We have studied a two-dimensional piecewise linear map to examine how the hierarchical structure of stable regions affects the slow dynamics in Hamiltonian systems. In the phase space there are infinitely many stable regions, each of which is polygonal-shaped, and the rest is occupied by chaotic orbits. By using symbolic representation of stable regions, a procedure to compute the edges of the polygons is presented. The stable regions are *hierarchically* distributed in phase space and the edges of the stable regions show the marginal instability. The cumulative distribution of the recurrence time obeys a power law as $\sim t^{-2}$, the same as the one for the system with phase space, which is composed of a single stable region and chaotic components. By studying the symbol sequence of recurrence trajectories, we show that the hierarchical structure of stable regions has no significant effect on the power-law exponent and that only the marginal instability on the boundary of stable regions is responsible for determining the exponent. We also discuss the relevance of the hierarchical structure to those in more generic chaotic systems.

I. INTRODUCTION

In phase space of generic Hamiltonian systems, regular and chaotic motions coexist [1–3]. Regular orbits form invariant curves on which the motion is quasiperiodic, while chaotic trajectories wander in the rest of phase space. In the vicinity of invariant tori, chaotic trajectories spend a long time before they eventually get away from tori [2,4,5]. Such *sticky* motions lead to nonexponential behavior of statistical quantities: for instance, in generic mixed phase space the distribution for Poincaré recurrences asymptotically obeys a power law. These sticky motions relevant to the power law have been thoroughly studied by using the standard map,

$$p' = p + \frac{K}{2\pi}\sin(2\pi q),$$
$$q' \equiv q + p' \mod 1, \tag{1}$$

where K is a parameter. While there are numerous studies for the standard map, the existence of the universality of the power law in generic mixed phase space is still under debate [6–11]. For both theoretical and numerical studies, the structure of mixed phase space is so complicated, in general, which prevents us from rigorous investigations.

Stability islands are believed to be hierarchically distributed in generic mixed phase space: a stability island is surrounded by smaller resonant islands, each of which is also surrounded again by smaller resonance islands. Assuming that the transition in a hierarchical structure takes place in a stochastic manner, Meiss and Ott have introduced a Markov tree model [12], in which the regions enclosed by cantori or partial barriers are taken as the nodes of the tree and the transition between nodes is modeled by a Markov process. Such an approach has stimulated subsequent works and now is one of promising platform for the issue [3,13]. While Meiss and Ott have proposed a model with hierarchical structures, this does not necessarily mean that the existence of the hierarchical structure is a necessary condition of the power law. Indeed, it has been

shown that the power law around the critical invariant torus can be attributable to self-similar Markov chains that differ from the hierarchical structures in the sense of Meiss and Ott [14].

Another strategy to examine the power law would be to employ sharply divided phase space in which the boundaries between regular and chaotic components are simple smooth curves/lines. In phase space of mushroom billiards [15–18] or a certain class of piecewise linear maps [19–21], chaotic trajectories stay for a long time along the boundary in spite of the absence of hierarchical structures. Due to the existence of the family of marginally unstable periodic orbits, the exponent for the recurrence time is shown to be $\nu = 2$ [21]. The result does not provide any insight into the universality of power-law exponents, since sharply divided phase spaces are not generic ones as those for the standard map. However, such an observation at least tells us that the existence of hierarchical structure is not a necessary condition to have power-law behaviors. In the present paper, we will look anew at the role of hierarchical structures by taking a rather tractable system with hierarchical phase space, which contains infinity stable islands of marginal instability, though still not generic enough, and promote our understanding of generic Hamiltonian systems.

II. THE PIECEWISE LINEAR MAP

Let us consider a linearized version of the standard map Eq. (1), replacing the sine function with a piecewise linear function, $S(q) = \{q\,(0 \leqslant q < 1/4), 1/4 - q\,(1/4 \leqslant q < 3/4), q - 1/2\,(3/4 \leqslant q < 1)$. By applying a coordinate transformation, the "linearized standard map" is shown to be equivalent to the following map on $\mathbb{T}^2 = [-1/2, 1/2]^2$:

$$x' \equiv y \mod 1,$$
$$y' \equiv \begin{cases} -x + (2+K)y - K/4 & (y \geqslant 0) \\ -x + (2-K)y - K/4 & (y < 0) \end{cases} \mod 1, \tag{2}$$

where K is a parameter. It has been proven that for $K \geqslant 4$ the system is almost hyperbolic [22], meaning that every point is decomposed into stable and unstable directions, but there exists no finite lower bounds for the angle between these
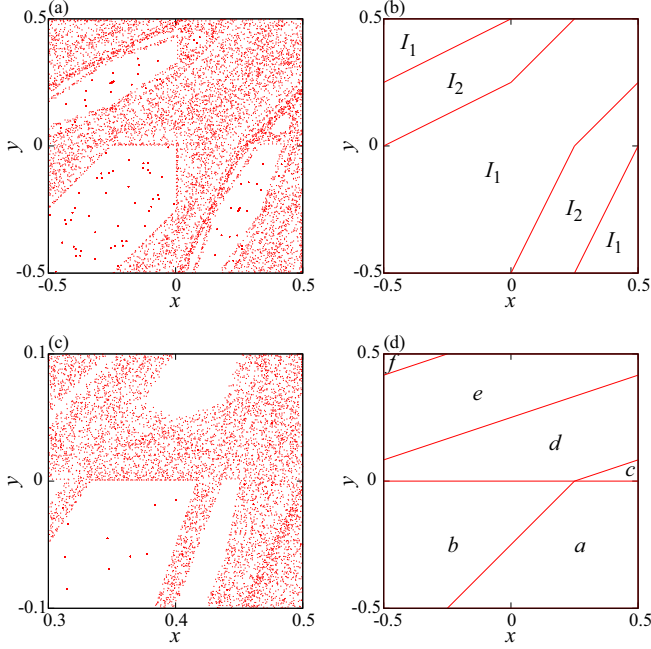
* akaishi@uec.ac.jp

FIG. 1. (a) Phase space portrait for the piecewise linear map with $K = 1$. (b) The two invariant domains are denoted by $\mathcal{I}_1$ and $\mathcal{I}_2$. The red lines indicate the boundary between these two regions. (c) Magnification of the phase-space portrait. (d) Phase space partitioning for the map (2) with $K = 1$. Each region is defined by the inequalities (4).

directions. Moreover, for $K = K_m := 2(1 + \sin(\frac{\pi}{m-1}))$ ($m = 2, 3, \ldots$) only a single stable region exists in phase space and the rest is chaotic [22]. The stable region forms a $2m$-sided polygon. Note that the stable region is a set of periodic orbits with an identical period depending on m, rather than a bundle of invariant tori whose rotation number continuously varies. The discussion of ergodic properties and stable regions for similar piecewise linear maps is found in Ref. [23].

For $0 < K < 4$ except K_m, phase space is a complicated mixture of stable and chaotic regions. In such generic cases, each stable region forms an ellipse in which the motion is quasiperiodic. Since the map is piecewise linear, the rotation number in each stable region is constant, unlike stable islands in generic mixed phase space. In this sense, our mapping system is not generic in the class of area-preserving maps.

In the present study, we focus on the case $K = 1$ and thus simply denote the map Eq. (2) with $K = 1$ by $(x', y') = F(x, y)$. As we will explain in the following sections, the phase space for $K = 1$ contains nontrivial hierarchical structure of stable polygonal regions and no stable ellipses that are composed of a bundle of invariant circles with irrational rotational numbers

The case of $K = 1$

Figure 1(a) illustrates a phase-space portrait for $K = 1$. One can easily show that the phase space is divided into two disjoint invariant domains, $\mathcal{I}_1$ and $\mathcal{I}_2$ [see Fig. 1(b)]. The domain $\mathcal{I}_1$ consists of a hexagonal-shaped stable region, which is located in the third quadrant, and a single ergodic component. In

contrast to the simple configuration of $\mathcal{I}_1$, stable regions in $\mathcal{I}_2$ are complex [see Fig. 1(c)]. In the region $\mathcal{I}_2$, it seems that infinite-many stability islands and a single chaotic component coexist.

The boundaries of stable regions both in $\mathcal{I}_1$ and $\mathcal{I}_2$ are marginally unstable. More precisely, a family of unstable periodic orbits with zero Lyapunov exponents exists on the boundaries of the stable regions. Due to this marginal instability, chaotic trajectories have the power law property, i.e., the recurrence-time distribution has an asymptotic power-law tail. We remark that the boundaries between $\mathcal{I}_1$ and $\mathcal{I}_2$ are also marginally unstable. Namely, the boundary lines are sets of marginally unstable periodic orbits (the existence of the boundary lines is also discussed in Ref. [24]). Therefore, in $\mathcal{I}_1$, the orbits stick along the boundary lines or the edges of polygonal shaped stable regions. On the other hand, $\mathcal{I}_2$ contains many sources of marginal instability and they form complex structures in phase space.

For convenience of the following analyses, we rewrite the map Eq. (2) without modulo arithmetic operations. First, we define six regions in phase space, labeled as $a, b, \ldots, f$ [see Fig. 1(d)], each of which is specified by the sets of inequalities,

$$R_s = \{(x, y) \mid \\ \text{the set of inequalities } I_s \text{ are satisfied.}\}, \quad (3)$$

where s represents one of the regions labeled by, $a, b, \ldots, f$, and the sets of inequalities are given as

$$I_a = \{y < 0, y > -1/2, x < 1/2, y < x - 1/4\},$$
$$I_b = \{y < 0, y > -1/2, x > -1/2, y > x - 1/4\},$$
$$I_c = \{y > 0, x < 1/2, y < x/3 - 1/12\},$$
$$I_d = \{y > 0, x > -1/2, x < 1/2,$$
$$\quad y > x/3 - 1/12, y < x/3 + 1/4\}, \quad (4)$$
$$I_e = \{y < 1/2, x > -1/2, x < 1/2,$$
$$\quad y > x/3 + 1/4, y < x/3 - 7/12\},$$
$$I_f = \{y < 1/2, x > -1/2, y > x/3 - 7/12\}.$$

Then, we define the map on R_s as

$$\begin{pmatrix} x' \\ y' \end{pmatrix} = F_s \begin{pmatrix} x \\ y \end{pmatrix} = M_s \begin{pmatrix} x \\ y \end{pmatrix} + V_s, \quad (5)$$

where

$$M_a = M_b = \begin{pmatrix} 0 & 1 \\ -1 & 1 \end{pmatrix},$$
$$M_c = M_d = M_e = M_f = \begin{pmatrix} 0 & 1 \\ -1 & 3 \end{pmatrix}, \quad (6)$$

$$V_a = \begin{pmatrix} 0 \\ 3/4 \end{pmatrix}, V_b = \begin{pmatrix} 0 \\ -1/4 \end{pmatrix}, V_c = \begin{pmatrix} 0 \\ 3/4 \end{pmatrix},$$
$$V_d = \begin{pmatrix} 0 \\ -1/4 \end{pmatrix}, V_e = \begin{pmatrix} 0 \\ -5/4 \end{pmatrix}, V_f = \begin{pmatrix} 0 \\ -9/4 \end{pmatrix}. \quad (7)$$

It is straightforward to check that the redefined map Eq. (5) with Eqs. (6) and (7) is equivalent to the original map Eq. (2) with $K = 1$.

FIG. 2. (a) Subregions for symbol length $n = 2$. The boundaries of the subregions are calculated by the procedure presented in the Appendix. (b) Subregions for $n = 3$. (c) The type of subregions for $n = 2$. There are only *hyperbolic* and *elliptic* regions. (d) The type of subregions for $n = 3$.

We remark that this partitioning is not a generating partition since the phase space is not fully chaotic. In fact, a single symbolic sequence is assigned to all the points in the stable polygonal domains.

III. PARTITION OF PHASE SPACE

The partition of phase space defined in the previous section naturally induces finer partitions. For a finite sequence of the symbols, $s_0 \ldots s_{n-1}$, where $s_i \in \{a, \ldots, f\}$, we define a region $R_{s_0 \ldots s_{n-1}}$ as

$$R_{s_0 \ldots s_{n-1}} = \{(x,y) \mid (x,y) \in R_{s_0}, \\ F(x,y) \in R_{s_1}, \ldots, F^{n-1}(x,y) \in R_{s_{n-1}}\}. \quad (8)$$

Since $R_{s_0 \ldots s_k} \in R_{s_0 \ldots s_{k-1}}$ the partition by all regions for $n = k$ is the subpartitioning of that for $n = k - 1$.

As shown in the Appendix, one can systematically calculate boundaries of the subregions. Since the coefficients for the inequalities Eq. (4), the matrix elements of Eq. (6) and the vectors Eq. (7) are rational numbers, the coordinates of vertices of subregions are rational numbers as well. Therefore, the computations of boundaries and vertices are free from numerical errors. In Fig. 2, the subregions for symbol sequences with symbol length 2 and 3 are shown. We can classify subregions according to their stability: each region $R_{s_0 \ldots s_{n-1}}$ is referred to either as *hyperbolic*, *elliptic*, or *parabolic*, according to the type of eigenvalues of its stability matrix,

$$M_{s_0 \ldots s_{n-1}} := \prod_{i=0}^{n-1} M_{s_i}. \quad (9)$$

TABLE I. Number of regions.

Length	Total	hyperbolic	elliptic	parabolic	identical
1	6	4	2	0	0
2	17	6	11	0	0
3	36	9	0	26	1
4	69	64	5	0	0
5	123	99	24	0	0
6	208	143	0	62	3
7	350	348	2	0	0
8	565	558	7	0	0
9	906	853	0	52	1
10	1465	1448	17	0	0
11	2374	2356	18	0	0
12	3878	3783	0	92	3
13	6335	6297	38	0	0
14	10367	10344	23	0	0
15	17128	17005	0	112	11
16	28323	28316	7	0	0
17	46859	46849	10	0	0
18	77508	77427	0	78	3

Note that all the elements of $M_{s_0 \ldots s_{n-1}}$ are integers. In addition, define *identical* regions if the matrix $M_{s_0 \ldots s_{n-1}} = \pm I$, where I is the identity map. Although the identical type is a special case of the parabolic type, we here distinguish these two types.

The number of subregions up to the symbol length 18 is listed in Table I. We note that the number of hyperbolic subregions exponentially increases with respect to the symbol length while that of the other types of subregions does not increase exponentially. Notice the parabolic (or identical) and elliptic regions appear in a complementary manner. The parabolic (or identical) regions only appear when the symbol length is given by integer multiples of 3, whereas the elliptic regions appear otherwise.

A. Stable regions

Identical regions are the "stable regions" that are described in Sec. II. Indeed, since the map for identical regions is the identity map, every point in the region is periodic with respect to the symbol length. The number of stable regions is not the same as the number of identical regions, namely, identical regions are multiply counted. For instance, the hexagonal stable region is labeled as *bbb* (see Fig. 2) and its *i*-repetition symbol sequence, denoted as $(bbb)^i$, represents the same stable region.

As mentioned above, identical regions are composed of the periodic orbits whose stability matrix is the identity matrix. Conversely, it follows that periodic points with identity stability matrix are contained in identical regions. One can make use of this fact to find stable regions: in fact, one can locate stable regions first by finding a periodic orbit with identity matrix, checking the symbolic sequence of the periodic orbit, then computing the boundaries of the region using the procedure in the Appendix. By applying such an algorithm, instead of enumerating all regions, we can find stable regions with long symbol length. Figure 3 shows the stable regions with symbol length 3, 6, 15, 33, 51, and 69. All
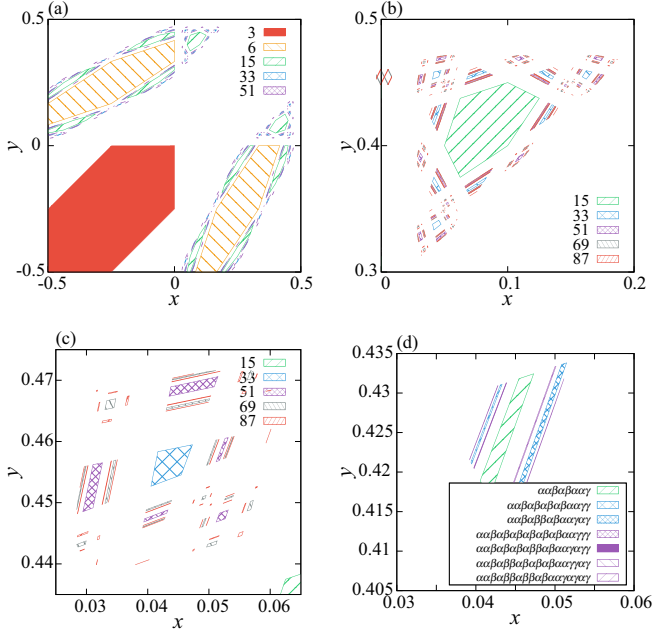
FIG. 3. (a) Stable regions with symbol length 3, 6, 15, 33, 51, 69, and 87. The number of the regions is 1, 2, 10, 66, 204, 552, and 1218, respectively. Except for symbol length 3 cases, every stable region has its symmetric one with respect to the line $x = y$. (b–d) Magnification of the stable regions. The stable regions are hierarchically aligned.

stable regions with symbol length 3, 6, 15 are hexagonal-shaped and for longer symbol sequences we have found only quadrilateral stable regions. One can clearly recognize self-similar patterns of the stable regions: for instance a stable region with symbol length 15 is surrounded by stable regions with length 33 and so on [see Fig. 3(b)]. Such a structure reminds us of the hierarchical structure of stable islands in generic mixed phase space.

Every stable region is "sticky" along its boundaries: one may expect that there is a family of marginally unstable periodic orbits on every edge of stable polygons [21]. In the neighborhood of the boundary of the stable regions, we have found the motion of chaotic trajectories is given as a constant shift along each boundary [20]. In fact, adjacent regions of the identical regions are parabolic. Note that the edges of the stable regions are also composed of periodic orbits. This means that the same type of marginal instability controls the stickiness in the map Eq. (2) with $K = K_m$. We emphasize that for the phase space with $K = 1$, there are numerous, possibly infinitely many, stable regions [25].

B. Symbol sequence

The self-similar pattern of stable regions in phase space is related to the symbol sequence of the regions. Identical regions have two properties in their symbol sequence. One is that the cyclic permutation of the symbol sequence of an identical region represents another identical region: if the region $R_{s_0 s_1 \ldots s_{n-1}}$ is identical, then $R_{s_1 \ldots s_{n-1} s_0}$ is identical as well. In fact, $R_{s_0 s_1 \ldots s_{n-1}}$ maps to $R_{s_1 \ldots s_{n-1} s_0}$ by a single iteration of the map. Another property concerns the reversed symbol sequence $s_{n-1} s_{n-2} \ldots s_0$. The region $R_{s_{n-1} s_{n-2} \ldots s_0}$ is an identical region for

TABLE II. Representative symbol sequences of stable regions. Symbols are expressed by the words defined in Eq. (10). The check mark above α indicates the words to be substituted by Eq. (11). The parentheses are inserted for readability.

Length	Word sequence
15	$\alpha\alpha\breve{\alpha}$
33	$\alpha\alpha(\beta\alpha\beta\breve{\alpha}\breve{\alpha}\gamma)$
51	$\alpha\alpha\beta\alpha\beta(\beta\alpha\beta\breve{\alpha}\breve{\alpha}\gamma)\alpha\gamma$, $\alpha\alpha\beta\alpha\beta\alpha(\beta\alpha\beta\breve{\alpha}\breve{\alpha}\gamma)\gamma$
69	$\alpha\alpha\beta\alpha\beta\beta\alpha\beta(\beta\alpha\beta\breve{\alpha}\breve{\alpha}\gamma)\alpha\gamma\alpha\gamma$,
	$\alpha\alpha\beta\alpha\beta\beta\alpha\beta\alpha(\beta\alpha\beta\breve{\alpha}\breve{\alpha}\gamma)\gamma\alpha\gamma$,
	$\alpha\alpha\beta\alpha\beta\alpha\beta\alpha\beta(\beta\alpha\beta\breve{\alpha}\breve{\alpha}\gamma)\alpha\gamma\gamma$,
	$\alpha\alpha\beta\alpha\beta\alpha\beta\alpha\beta\alpha(\beta\alpha\beta\breve{\alpha}\breve{\alpha}\gamma)\gamma\gamma$
87	$\alpha\alpha\beta\alpha\beta\beta\alpha\beta\beta\alpha\beta(\beta\alpha\beta\breve{\alpha}\breve{\alpha}\gamma)\alpha\gamma\alpha\gamma\alpha\gamma$,
	$\alpha\alpha\beta\alpha\beta\beta\alpha\beta\beta\alpha\beta\alpha(\beta\alpha\beta\breve{\alpha}\breve{\alpha}\gamma)\gamma\alpha\gamma\alpha\gamma$,
	$\alpha\alpha\beta\alpha\beta\beta\alpha\beta\alpha\beta\alpha\beta(\beta\alpha\beta\breve{\alpha}\breve{\alpha}\gamma)\alpha\gamma\gamma\alpha\gamma$,
	$\alpha\alpha\beta\alpha\beta\beta\alpha\beta\alpha\beta\alpha\beta\alpha(\beta\alpha\beta\breve{\alpha}\breve{\alpha}\gamma)\gamma\gamma\alpha\gamma$,
	$\alpha\alpha\beta\alpha\beta\alpha\beta\alpha\beta\beta\alpha\beta(\beta\alpha\beta\breve{\alpha}\breve{\alpha}\gamma)\alpha\gamma\alpha\gamma\gamma$,
	$\alpha\alpha\beta\alpha\beta\alpha\beta\alpha\beta\alpha\beta\alpha\beta(\beta\alpha\beta\breve{\alpha}\breve{\alpha}\gamma)\alpha\gamma\gamma\gamma$,
	$\alpha\alpha\beta\alpha\beta\alpha\beta\alpha\beta\alpha\beta\alpha(\beta\alpha\beta\breve{\alpha}\breve{\alpha}\gamma)\gamma\gamma\gamma$

which the original region $R_{s_0 s_1 \ldots s_{n-1}}$ is symmetric with respect to the line $x = y$ [see Fig. 3(a)]. This follows from the fact that the inverse map of Eq. (2) is given by exchanging x and y of the original map with each other. Note that this property is also discussed in the literature [22,23].

Due to these two properties, a set of the stable regions obtained by cyclic permutation and inversion of symbol sequences is represented by a single symbol sequence. We regard such stable regions as a single group, represented by a single symbol sequence. Indeed, for symbol lengths 15, 33, 51, 69, and 87, the number of the region groups is assigned, respectively, as 1, 1, 2, 4, and 7. The representative symbol sequence of the groups are found to be reproduced by the following two rules:

(A) *The representative symbol sequence is composed of the three "words"*

$$\alpha : eaead,$$
$$\beta : ead, \qquad (10)$$
$$\gamma : ec.$$

(B) *In a symbolic sequence, the next generation in the hierarchy is generated from the previous generation by substituting words as*

$$\alpha \rightarrow \beta\alpha\beta\alpha\alpha\gamma. \qquad (11)$$

Table II lists the word representation of the stable regions. We note, in rule (B), that only the α's indicated by the check marks in Table II are substituted to generate the next generation.

IV. RECURRENCE TIME DISTRIBUTION

Recurrence time statistics is often studied to characterize the stickiness of chaotic trajectories. The recurrence-time distribution $P(t)$ is defined as the probability to return to a given recurrence region at time t. Instead of the raw distribution, we here use the cumulative distribution
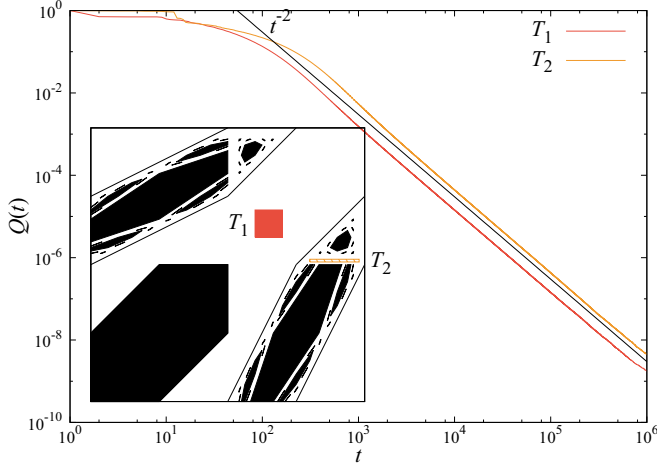
FIG. 4. Cumulative recurrence-time distributions. The inset shows the phase space and the recurrence regions. The recurrence region T_1 is a rectangular ($0.1 \leqslant x \leqslant 0.2, 0.1 \leqslant y \leqslant 0.2$) and T_2 is ($0.3 \leqslant x \leqslant 0.48, 0.01 \leqslant y \leqslant 0.02$). T_1 is contained in $\mathcal{I}_1$ and T_2 in $\mathcal{I}_2$. The recurrence regions are chosen so as not to overlap any stable regions.

$Q(t) := \sum_{t'=t}^{\infty} P(t')$, that is the probability to return for the time longer than t.

Figure 4 shows the cumulative distribution of the recurrence time, for which we take two recurrence regions. The recurrence region T_1 is put in the chaotic component in $\mathcal{I}_1$ and T_2 is put in $\mathcal{I}_2$ (see the inset of Fig. 4). One can clearly see that the distribution obeys the power law:

$$Q(t) \sim t^{-2}. \tag{12}$$

It should be noted that the power law exponent takes the same value as the one for $K = K_m$ not only for the region $\mathcal{I}_1$ but also for $\mathcal{I}_2$. This means that although in $\mathcal{I}_2$ many stable regions are hierarchically distributed, the exponent for the recurrence-time distribution is not affected

In order to investigate the power law found in the recurrence-time distribution, it would be helpful to observe the itinerary before the orbit returns to a recurrence region. Since the stickiness originates from marginally unstable periodic orbits, orbits with large recurrence time stay in the region close to these sticky regions in phase space for a long time. Indeed, as shown in Fig. 5, typical orbits leaving the recurrence region T_1 have relatively long recurrence time and stick along the boundaries of the stable hexagonal or along the boundary lines between $\mathcal{I}_1$ and $\mathcal{I}_2$. Similarly, in $\mathcal{I}_2$ the boundary lines and stable regions seem to attract recurrent orbits for a long time. These observations are basically consistent with those in sharply divided phase space with a single stable region.

A. Symbol statistics

In order to clarify whether the hierarchical structure is relevant to the stickiness, one needs to quantify how long recurrent orbits get stuck around stable regions. For this purpose, we use symbol representation of recurrent orbits: for each initial point of a given recurrent orbit, we define the corresponding symbol sequence in such a way that the
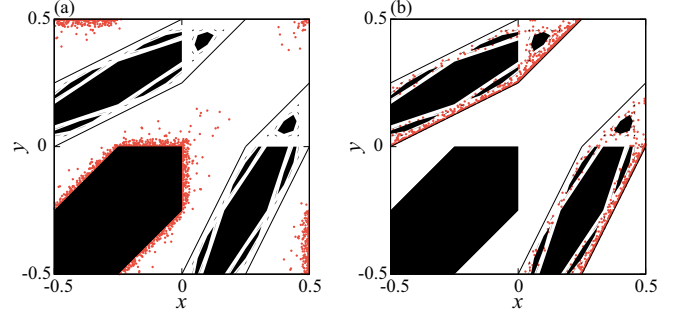
FIG. 5. A typical recurrence orbit for (a) the recurrence region T_1 and for (b) T_2. Stable regions are shown as filled black polygons. The recurrence time of the orbits is 1148 for (a) and 1044 for (b).

symbols of the region that the orbit visits are concatenated in its visiting order. The length of the symbol sequence is equal to the recurrence time of the orbit. Needless to say, the symbol representation allows one to see each orbit in "coarse-grained" phase space. For instance if the symbol sequence of an orbit has the subsequence represented as $\dots ead \dots$, the orbit visits the region of the subsequence, R_{ead}, when such a subsequence appears in the symbol sequence.

We here define symbol sequence statistics of recurrent orbits. For a given subsequence $\boldsymbol{s} = s_1 \dots s_l$ and a given initial point (x_0, y_0), let $\tau_{\boldsymbol{s}}(x_0, y_0)$ be the number of times the subsequence $s_1 \dots s_l$ appears in the symbol sequence of the orbit from the initial point (x_0, y_0) until the recurrence. Then let us define the symbol sequence statistics as

$$S_{\boldsymbol{s}}(\tau) = \text{Prob.}\big\{(x_0, y_0) \text{ such that } \tau_{\boldsymbol{s}}(x_0, y_0) > \tau \big\}. \tag{13}$$

In other words, $S_{\boldsymbol{s}}(\tau)$ is the probability of the recurrent orbits for which the subsequence $\boldsymbol{s}$ appears more than τ times. The quantity $S_{\boldsymbol{s}}(\tau)$ represents, for a given recurrence region, how many times recurrent orbits visit the region labeled by the symbol sequence $\boldsymbol{s}$. It could be a measure to see which phase-space regions are sticky.

First, we examine $S_{\boldsymbol{s}}(\tau)$ in $\mathcal{I}_1$. Figure 6 shows the symbol sequence statistics for the case where we take the recurrence region T_1. One can clearly find that the symbol sequence statistics exhibits two types of distributions: one obeys a power law and the other exponentially decays, depending on the symbol sequences. Note that the exponent of the power law is the same as the one for the recurrence time, namely $S(\tau) \sim \tau^{-2}$. This observation is consistent with the fact that the recurrent orbits stay long time only in sticky regions.

In order to classify symbol sequences, let here $\mathcal{F}_{s_1 \dots s_l}^{(m)}$ be the family of subsequences of length m in the infinite repetition of $s_1 \dots s_l$, namely,

$$\mathcal{F}_{s_1 \dots s_l}^{(m)} = \left\{ t_1 \dots t_m \;\middle|\; \begin{array}{l} t_i = t_{i+l}, i = 1, \dots, l \\ t_i = s_{i+j \,(\text{mod}\, l)}, j = 1, \dots, l \end{array} \right\},$$

Then, let us define the family of symbol sequences as $\mathcal{F}_{s_1 \dots s_l} = \bigcup_{m=l}^{\infty} \mathcal{F}_{s_1 \dots s_l}^{(m)}$, e.g., $\mathcal{F}_a = \{a, aa, aaa, \dots\}$, $\mathcal{F}_{ab} = \{ab, ba, aba, bab, \dots\}$, and so on. By observing the symbol sequences, we have found that only two families, $\mathcal{F}_{ead}(\mathcal{F}_{dae})$ and $\mathcal{F}_{afabdb}$, yield the power-law distribution. For the symbol sequences that are not contained in these two families, the symbol sequence statistics exhibits exponentially decaying
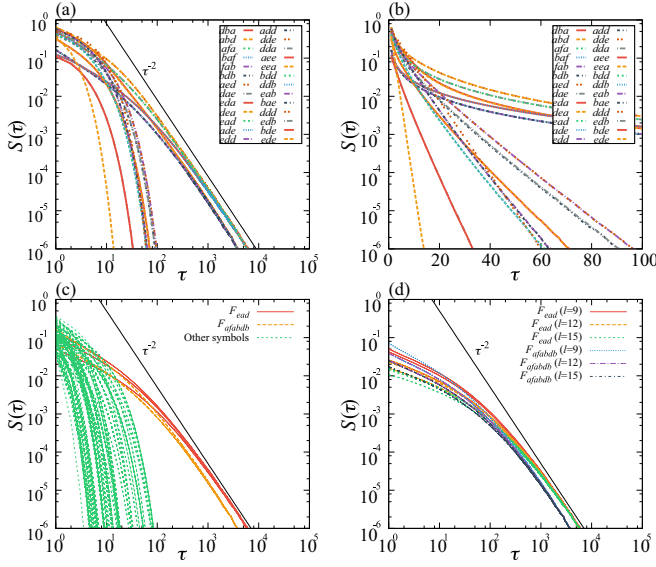
FIG. 6. (a) Symbol sequence statistics $S(\tau)$ for the recurrence region T_1. The length of the symbol sequences is 3. 26 symbol sequences are depicted. (b) Semilogarithmic plot of (a). (c) Symbol sequence statistics for the symbol sequence of length 6. The symbol sequences for the power law are classified into two groups, $\mathcal{F}_{ead} = \{eadead, adeade, deadea, daedae, edaeda, eadead\}$ and $\mathcal{F}_{afabdb} = \{afabdb, bafabd, dbafab, bdbafa, abdbaf, fabdba\}$. (d) Symbol statistics for $\mathcal{F}_{ead}$ ($\mathcal{F}_{dae}$) and $\mathcal{F}_{afabdb}$ with several symbol lengths. As the symbol length increases, the symbol statistics asymptotically approaches a power-law tail. The prefactor for the power law tail for $\mathcal{F}_{ead}$ is slightly greater than the one for $\mathcal{F}_{afabdb}$.

behavior [see Figs. 6(b) and 6(c)]. In Fig. 6(d), we show $S(\tau)$ by changing the length of the symbol sequence. Here, $\mathcal{F}_s(l)$ indicates the subset of $\mathcal{F}_s$ for the symbol length l. As the symbol length increases, meaning that "phase-space resolution" becomes higher, the power-law distribution becomes clear.

As explained in the previous sections, in $\mathcal{I}_1$ there are two sets of marginally unstable periodic orbits: the boundaries of the stable hexagonal R_{bbb} and the boundary between $\mathcal{I}_1$ and $\mathcal{I}_2$. Figure 7 demonstrates the phase-space regions in which the power-law behavior is found in the symbol sequence statistics. The orbits associated with the families of subsequence $\mathcal{F}_{eac}$ and $\mathcal{F}_{afabdb}$, respectively, stick along the boundary lines between $\mathcal{I}_1$ and $\mathcal{I}_2$ and the boundaries of the stable region R_{bbb}.

In this way, we confirm that the symbol sequence statistics $S_s(\tau)$ could be a measure to know which region is responsible for the power law of the recurrence time. The asymptotic behavior of $S_s(\tau)$ therefore becomes as

$$S_s(\tau) \sim \begin{cases} \tau^{-2} & R_s \text{ is a "sticky" region} \\ \exp(-k_s\tau) & \text{otherwise} \end{cases}, \quad (14)$$

where k_s is a coefficient for exponential decay.

B. The power-law decay in $\mathcal{I}_2$

We next investigate the symbol sequence statistics for the invariant set $\mathcal{I}_2$ that contains hierarchical stable islands. Figure 8 shows the symbol sequence statistics in the case where T_2 is taken as the recurrence region. Similar to the results for $\mathcal{I}_1$,
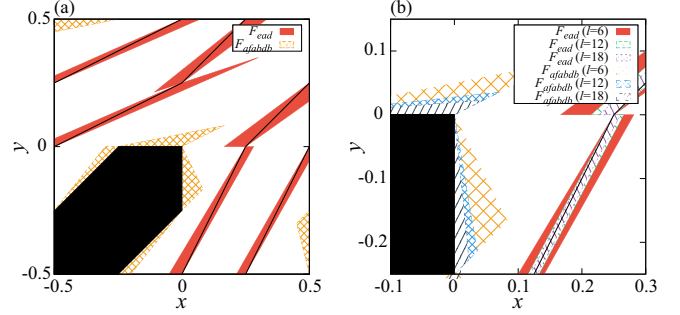

FIG. 7. (a) Phase-space regions in which the power-law behavior is found in the symbol sequence statistics. The black filled hexagon represents the stable region and the boundary lines between $\mathcal{I}_1$ and $\mathcal{I}_2$ are indicated by the black lines. (b) Magnification of panel (a). The regions with different symbol length are overlaid. As the symbol length l increases, the region of $\mathcal{F}_{ead}$ shrinks into the boundary lines. For $\mathcal{F}_{afabdb}$ the region shrinks into the hexagon edges as the symbol length increases.

the statistics exhibits the asymptotic power law $S_s(\tau) \approx C\tau^{-2}$ for particular symbol sequences. In this case, we found that the four families, $\mathcal{F}_{ead}$, $\mathcal{F}_{ceaeadedaeae}$, $\mathcal{F}_{\alpha\alpha\beta\gamma}$, and $\mathcal{F}_{\alpha\alpha\beta\alpha\beta\beta\gamma\alpha\gamma}$, are responsible for the power law. For the rest of the symbol sequences, due to the limitation of computational resources to obtain statistically reliable data, we could not judge whether power-law tails appear or not (while some of those clearly exhibit exponential decays). Note that the exponent of the power-law decay for these families is 2, meaning that the existence of hierarchical stability islands does not seem to play any significant role.

The orbits associated with such families, as shown in Fig. 9, stay in the vicinity of the stable regions to which the corresponding symbols of families are assigned. As seen in the previous subsection, the regions for $\mathcal{F}_{ead}$ are located along the boundary lines between $\mathcal{I}_1$ and $\mathcal{I}_2$. The regions for $\mathcal{F}_{ceaeadedaeae}$ are along the boundaries of the two stable
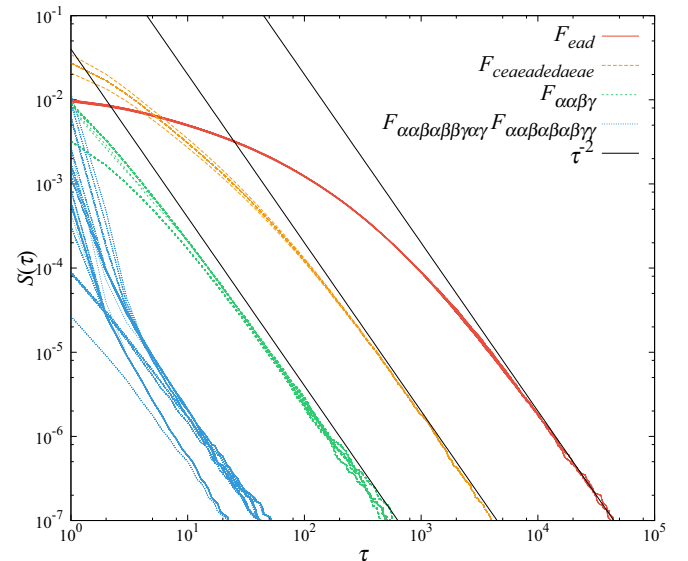

FIG. 8. Symbol statistics for the recurrence region T_2. The symbol length is 39. The number of initial points is taken as 10^8.
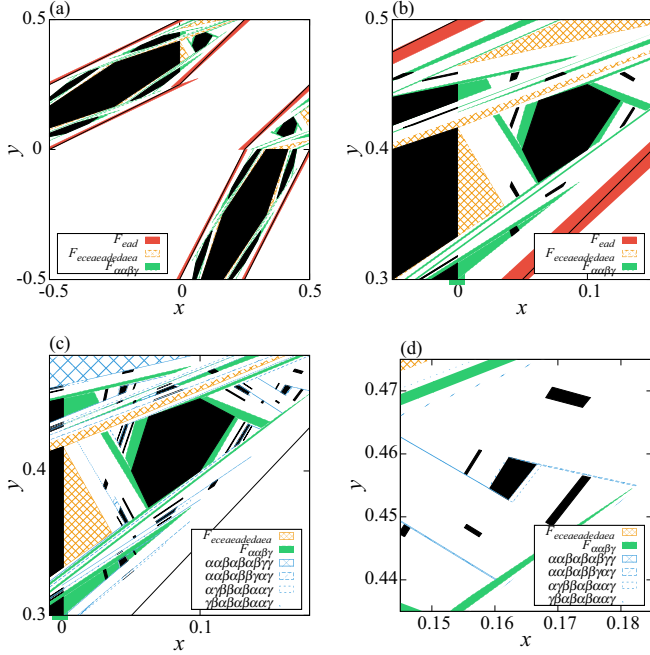
FIG. 9. Phase space regions in which the power-law behavior is found in the symbol sequence statistics. (a) The whole phase space. From (b) and (c) to (d), we gradually magnify hierarchical regions. The black filled polygons show stable regions.

hexagonal regions R_{eaeaea}. The regions for the families $\mathcal{F}_{\alpha\alpha\beta\gamma}$ and $\mathcal{F}_{\alpha\alpha\beta\alpha\beta\beta\gamma\alpha\gamma}$ are located at the boundaries of the stable regions $R_{\alpha\alpha\alpha}$ and $R_{\alpha\alpha\beta\alpha\beta\alpha\alpha\gamma}$, respectively.

We remark that these word sequences are the first two levels in the hierarchy of the stable regions (see Table II). These facts ensure that the power-law decay of the recurrence time originates from the marginal instability of the boundary of the stable regions. In our numerical observations, the motion of transitions between different levels in the hierarchy is not responsible for the power law. The marginal instability is only the source of the stickiness and the existence of hierarchy of stability islands does not affect the power law of the recurrence.

For the four families exhibiting the power-law decay of the symbol sequence statistics, the prefactor of the decay C significantly differs between the hierarchy levels, while the exponent is the same (see Fig. 8). The magnitude of the prefactor manifests the probability of how often orbits enter each sticky region. Assuming that the injection probability is proportional to the area of the sticky region in phase space, it is consistent that the magnitude of the prefactor value decreases as the level of hierarchy increases. With increase in the hierarchy level, the size of stable regions becomes smaller and thus the area of sticky regions is reduced, whereas the number of stable regions increases, at most, algebraically. The largest sticky region plays a significant role to the power-law decay of the recurrence-time distribution.

V. CONCLUSION AND DISCUSSION

We have investigated the influence of hierarchical structure of stable regions on the recurrence-time statistics by closely examining the phase-space structure of the piecewise linear map (2) with $K = 1$. The phase space is composed of two invariant domains: one contains a single stable region and the other infinitely many stable regions. Each stable region is composed of a set of periodic orbits and forms a convex polygon. By rewriting the original map into the form without modulo arithmetic operation, we could introduce a proper partition in phase space, which leads a kind of symbolic dynamics. Such a symbolic dynamics allows us to find the one-to-one correspondence between single symbol sequences and stable islands. This also offers an efficient systematic procedure to compute the edges of stable polygons. We have shown that the stable regions form a hierarchical structure: stable regions in each hierarchy level is surrounded by those of the next hierarchical level and so on. Moreover, we have confirmed that the symbol sequences of stable regions have a certain relationship among different hierarchy levels. Namely, symbol sequences in a hierarchy level is generated from the ones in the lower level by replacing specific symbol sequences by other ones. This relation in the symbol expression is closely linked to the fact that the stable islands form the hierarchical structure in phase space.

We have examined how the hierarchical structure affects the recurrence-time distribution. The most important finding is that the power-law exponent does not depend on whether or not there exists the hierarchical structure of stable regions. On the boundaries of stable regions one may expect there exists a family of marginally unstable periodic orbits. Due to the marginal instability, the exponent for the recurrence time becomes $\nu = 2$, as is the case of the map Eq. (2) with K_m or the case of the stadium and mushroom billiards. We note that the mapping with $K = 1$ belongs to a special class of dynamical systems in spite of the existence the hierarchical structure.

To verify that recurrent orbits are sticky only close to the boundaries of stable regions, we have introduced the symbol sequence statistics for recurrent orbits, based on the symbolic expression of the orbits. The symbol statistics represents how many times orbits visit a given region in phase space until the recurrence occurs. For the regions close to stable regions, the symbol statistics exhibits a power law tail, $S(\tau) \approx C\tau^{-2}$, where the exponent is exactly the same value as that given in the recurrence time. In each hierarchy level, the statistics obeys the same power law, while the prefactor C differs among the hierarchy levels. The prefactor tends to be smaller as the size of the stable regions becomes smaller.

In generic phase space, as mentioned in the introduction section, there have been discussions on the origin of power law decay in generic mixed systems. A model introduced by Meiss and Ott assumes a hierarchical structure of islands of stability, and the transition among different hierarchical levels is considered to invoke the power-law decay. However, for the present piecewise linear map, the existence of hierarchy does not play any role, but only the power law originates solely from the marginal instability around each stable region. Such difference originates from the difference in configurations of sticky regions, which is schematically shown in Fig. 10. In our sharply divided hierarchical phase space, only the vicinity of stable regions is sticky and different sticky regions do not overlap in phase space with each other. In generic cases, on the other hand, the resonant stable islands are located in the parent's sticky region so that the surrounding sticky regions form hierarchical structures and thus the transitions among several hierarchy levels are critical to the long-time sticky
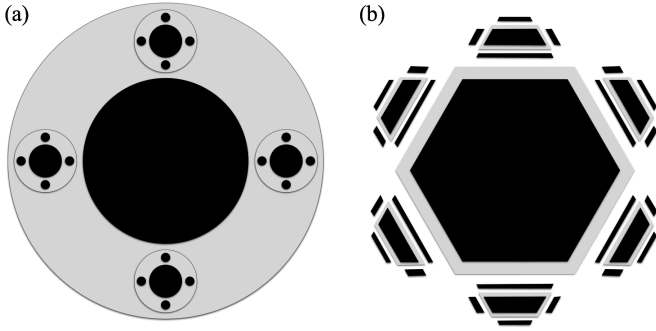
(a) (b)

FIG. 10. Schematics picture of the hierarchical structures in (a) generic mixed phase space and in (b) our sharply divided mixed phase space. The black regions indicate the stable regions and the gray ones indicate the surrounding sticky regions.

motions. For this reason, the present result might not be directly linked to the universality in generic situations discussed so far, but it tells us that not only hierarchical structure of stable islands but also configuration of sticky regions are significant for the power-law decay.

APPENDIX: A PROCEDURE TO COMPUTE PHASE-SPACE PARTITIONS

We here present a procedure to compute the partition of phase space. The partition is generated by iterating the piecewise linear map, which is defined on n subregions in phase space independently and affine in each region.

Let n be the number of regions and $S = \{s_1, \ldots, s_n\}$ be a set of symbols and R_{s_i} be a convex polygon region on the two-dimensional plane. Each convex polygon, R_s for $s \in S$, is expressed by a set of inequalities as

$$R_s = \left\{ (x,y) \in \mathbf{R}^2 \mid \begin{array}{c} a_s^{(1)}x + b_s^{(1)}y > c_s^{(1)} \\ \vdots \\ a_s^{(m_s)}x + b_s^{(m_s)}y > c_s^{(m_s)} \end{array} \right\}, \quad \text{(A1)}$$

where m_s is the edge number of the polygon and the coefficients $a_s^{(j)}, b_s^{(j)}, c_s^{(j)}$ specify the edge lines.

Assuming that $R_{s_i} \cap R_{s_j} = \emptyset$ for $i \neq j$, let us define a piecewise linear map on $\sum_i \bigcup R_{s_i}$, $(x', y') = F(x,y)$, as

$$\begin{pmatrix} x' \\ y' \end{pmatrix} = \begin{cases} M_{s_1} \begin{pmatrix} x \\ y \end{pmatrix} + V_{s_1} & (x,y) \in R_{s_1} \\ \vdots & \\ M_{s_n} \begin{pmatrix} x \\ y \end{pmatrix} + V_{s_n} & (x,y) \in R_{s_n} \end{cases}, \quad \text{(A2)}$$

where M_i is a matrix and V_i is a vector. The regions R_{s_i} form a fundamental phase-space partition for the map.

For a given finite symbol sequence $t_0 \ldots t_k$ where $t_i \in S$, let us define a subregion as

$$R_{t_0 \ldots t_k} = \left\{ (x,y) \in \mathbf{R}^2 \mid \begin{array}{c} (x,y) \in R_{t_0} \\ F(x,y) \in R_{t_1} \\ \vdots \\ F^k(x,y) \in R_{t_k} \end{array} \right\}. \quad \text{(A3)}$$

Since each region is defined by a set of inequalities, the conditions for $R_{t_0 \ldots t_k}$ are expressed by inequalities as well. Namely, one of the inequalities for the condition $F^i(x,y) \in R_{t_i}$ in Eq. (A3) is

$$\left(a_{t_i}^{(j)} \, b_{t_i}^{(j)} \right) \cdot \begin{pmatrix} x_i \\ y_i \end{pmatrix} > c_{t_i}^{(j)}, \quad \text{(A4)}$$

where

$$\begin{pmatrix} x_i \\ y_i \end{pmatrix} = \left(\prod_{p=0}^{i-1} M_{t_p} \right) \begin{pmatrix} x \\ y \end{pmatrix} + \sum_{p=0}^{i-1} \left(\prod_{q=p+1}^{i-1} M_{t_q} \right) V_{t_p}. \quad \text{(A5)}$$

To obtain a subregion, it is sufficient to check whether all these inequalities are satisfied simultaneously. If these inequalities are not satisfied simultaneously, the region for the symbol sequence no longer exists in phase space. One can compute the edges and the vertices of the subregion by reducing the inequalities into the minimal ones.

[1] C. F. F. Karney, Physica D (Amsterdam) **8**, 360 (1983).

[2] B. V. Chirikov and D. L. Shepelyansky, Physica D (Amsterdam) **13**, 395 (1984).

[3] J. D. Meiss, Rev. Mod. Phys. **64**, 795 (1992).

[4] B. V. Chirikov and D. L. Shepelyansky, Phys. Rev. Lett. **82**, 528 (1999).

[5] M. Weiss, L. Hufnagel, and R. Ketzmerick, Phys. Rev. Lett. **89**, 239401 (2002).

[6] G. Cristadoro and R. Ketzmerick, Phys. Rev. Lett. **100**, 184101 (2008).

[7] E. G. Altmann and T. Tél, Phys. Rev. E **79**, 016204 (2009).

[8] R. Venegeroles, Phys. Rev. Lett. **102**, 064101 (2009).

[9] R. Ceder and O. Agam, Phys. Rev. E **87**, 012918 (2013).

[10] C. V. Abud and R. E. de Carvalho, Phys. Rev. E **88**, 042922 (2013).

[11] O. Alus, S. Fishman, and J. D. Meiss, Phys. Rev. E **90**, 062923 (2014).

[12] J. D. Meiss and E. Ott, Phys. Rev. Lett. **55**, 2741 (1985).

[13] J. D. Meiss, Chaos **25**, 097602 (2015).

[14] J. Hanson, J. Cary, and J. Meiss, J. Stat. Phys. **39**, 327 (1985).

[15] E. G. Altmann, A. E. Motter, and H. Kantz, Chaos **15**, 033105 (2005).

[16] T. Miyaguchi, Phys. Rev. E **75**, 066215 (2007).

[17] S. Tsugawa and Y. Aizawa, J. Phys. Soc. Jpn. **81**, 064004 (2012).

[18] L. A. Bunimovich, J. Stat. Phys. **154**, 421 (2014).

[19] J. Malovrh and T. Prosen, J. Phys. A **35**, 2483 (2002).

[20] E. G. Altmann, A. E. Motter, and H. Kantz, Phys. Rev. E **73**, 026207 (2006).

[21] A. Akaishi and A. Shudo, Phys. Rev. E **80**, 066211 (2009).

[22] M. Wojtkowski, Commun. Math. Phys. **80**, 453 (1981).

[23] M. Wojtkowski, Ergod. Theory Dyn. Syst. **2**, 525 (1982).

[24] S. Bullett, Commun. Math. Phys. **107**, 241 (1986).

[25] K. Aoki, A. Akaishi, and A. Shudo (unpublished).